

# Water Vapor and Hydrogen in the Terrestrial Planet Forming Region of a Protoplanetary Disk

J.A. Eisner

<sup>1</sup>*Department of Astronomy, 601 Campbell Hall, University of California, Berkeley, CA 94720*

Planetary systems, ours included, are formed in disks of dust and gas around young stars. Disks are an integral part of the star and planet formation process<sup>1,2</sup>, and knowledge of the distribution and temperature of inner disk material is crucial for understanding terrestrial planet formation<sup>3</sup>, giant planet migration<sup>4</sup>, and accretion onto the central star<sup>5</sup>. While the inner regions of protoplanetary disks in nearby star forming regions subtend only a few nano-radians, near-IR interferometry has recently enabled the spatial resolution of these terrestrial zones. Most observations have probed only dust<sup>6</sup>, which typically dominates the near-IR emission. Here I report spectrally dispersed near-IR interferometric observations that probe gas (which dominates the mass and dynamics of the inner disk), in addition to dust, within one astronomical unit of the young star MWC 480. I resolve gas, including water vapor and atomic hydrogen, interior to the edge of the dust disk; this contrasts with results of previous spectrally dispersed interferometry observations<sup>7,8</sup>. Interactions of this accreting gas with migrating planets may lead to short-period exoplanets like those detected around main-sequence stars<sup>4</sup>. The observed water vapor is likely produced by the sublimation of migrating icy bodies<sup>9</sup>, and provides a potential reservoir of water for terrestrial planets<sup>10</sup>.

I obtained observations with a new grism<sup>11</sup> (a dispersive element consisting of a diffraction

grating on the vertex of a prism) at the Keck Interferometer<sup>12,13</sup> that show, for the first time, evidence of spatially resolved gaseous spectral-line emission interior to the edge of the dusty disk around a young star, MWC 480. My observations provide a spectral dispersion of  $R = 230$  from 2.0 to 2.4  $\mu\text{m}$  wavelength, and an angular resolution of approximately 1 milli-arcsecond (mas; 1 mas  $\approx$  5 nano-radians), which is  $\sim 0.1$  astronomical units (AU) at the 140 parsec distance to the target (the source is located in the Taurus-Auriga star forming complex). MWC 480 has a stellar mass of  $2.3 M_{\odot}$ , an age of  $\sim 6$  Myr, and a circumstellar disk of dust and gas in Keplerian rotation<sup>14</sup>. Previous observations found that the dusty component of the disk extended to within  $\sim 0.5$  AU of the central star<sup>15,16</sup>, and suggested the presence of hot gaseous emission at even smaller stellocentric radii<sup>17</sup>. My observations confirm these suggestions, and resolve hydrogen gas and water vapor in the inner disk.

My interferometry data provide a measurement of the angular size of the circumstellar emission from MWC 480 as a function of wavelength (Figure 1). The spectral dependence of the angular size indicates a radial temperature gradient. Since cooler material emits relatively more radiation at longer wavelengths, an outwardly decreasing temperature gradient yields an increasing fraction of emission from larger radii, and hence a larger angular size, at longer wavelengths. The temperature gradient probably arises from multiple components at different stellocentric radii<sup>17</sup>: warm dust at radii where temperatures approach the dust sublimation temperature, and hotter gas at smaller radii.

Figure 1 also shows more compact emission at 2.165  $\mu\text{m}$  relative to the surrounding con-

tinuum. This dip corresponds to the wavelength of the  $\text{Br}\gamma$  electronic transition ( $n = 7 \rightarrow 4$ ) of hydrogen. The  $\text{Br}\gamma$  emission observed from MWC 480 traces very hot gas ( $\sim 10^4$  K) that has recently recombined from ionized hydrogen<sup>18</sup>, presumably in the inner reaches of an accretion column.

To match the features of Figure 1, I constructed a simple physical model and fitted it directly to the measured  $V^2$  and fluxes. The model accounts for emission of the unresolved central star, circumstellar continuum emission from hot gas, spectral-line emission from hydrogen ( $\text{Br}\gamma$ ), and continuum emission from warm dust. I take each emission component to be a uniform ring whose width is 20% of its radius. This multiple-ring model approximates a continuous disk where dust, gas, and individual gaseous atoms or molecules contribute emission at different size scales. It has been shown previously that ring models provide reasonable approximations to more complex models of inner disk regions<sup>15,19</sup>. I also assume that the gaseous continuum and  $\text{Br}\gamma$  emission originate from stellocentric radii smaller than 0.1 AU; given the  $\sim 1$  mas angular resolution of my observations, I can not accurately distinguish between smaller radii, although I can rule out larger radii.

As indicated in Figure 2, the model fits the data well over most of the spectral bandpass. However, there are substantial deviations between the model predictions and the data in the region between 2.0 and 2.1  $\mu\text{m}$  (particularly for the fluxes). These deviations suggest the presence of hot water vapor, which has substantial opacity from 2.0 to 2.1  $\mu\text{m}$ , in the inner disk of MWC 480. I include water vapor in the model by adding a ring of material with the opacity of water vapor<sup>20</sup>.

The superior quality of the fit when water is included clearly demonstrates the presence of H<sub>2</sub>O in the inner disk of MWC 480 (for further arguments why the model must include water vapor emission in order to match the data, see the Supplementary Information section).

The best-fit model includes compact gaseous continuum emission with a temperature of  $2410 \pm 125$  K and Br $\gamma$  emission that adds  $17\% \pm 7\%$  to this gaseous continuum flux at  $2.165 \mu\text{m}$ ; these components are situated at stellocentric radii  $< 0.1$  AU. Water vapor emission is located at a radius of  $0.16 \pm 0.05$  AU. The temperature of this material is  $2300 \pm 120$  K and the column density is  $1.2 \pm 0.6 \times 10^{19} \text{ cm}^{-2}$ . Dust emission originates from a radius of  $0.28 \pm 0.01$  AU and has a temperature of  $1200 \pm 60$  K. Quoted  $1\sigma$  uncertainties are quadrature sums of statistical uncertainties in the fits and assumed 5% systematic errors.

I illustrate the basic geometry of the innermost regions of MWC 480 in Figure 3. As inferred from the data, gaseous emission is found at substantially smaller stellocentric radii than the dust. The inner edge of the dust disk lies at  $\sim 0.3$  AU, where the disk temperature approaches the sublimation temperature of silicate dust<sup>21</sup>. Because I also include contributions from gas in my analysis, the inferred dust size is larger, and the temperature lower, than in previous work where only dust emission was considered<sup>15,16</sup>. Emission from H<sub>2</sub>O is found at  $\sim 0.15$  AU, and hot gaseous continuum and Br $\gamma$  emission at still smaller radii ( $< 0.1$  AU). The observed Br $\gamma$  emission probably originates in an accretion column, near the shock formed when infalling material impacts high latitude regions of the star<sup>5,22,23</sup>.

My results substantiate models of inner disk structure proposed previously for similar star+disk

systems<sup>24</sup>. Comparison with these models suggests that in order to reproduce the ratio of flux in the gas and dust components determined here ( $\sim 0.5$ ), a mass accretion rate  $\gtrsim 10^{-7} \text{ M}_{\odot} \text{ yr}^{-1}$  must be invoked for MWC 480. At such high accretion rates, the inner disk gas becomes optically thick to its own radiation, and can therefore produce relatively more flux. Furthermore, models with this high accretion rate produce strong  $\text{Br}\gamma$  emission, consistent with my detection. My measurement of gas interior to the edge of the dust disk also confirms previous suggestions of such structure based on modeling of spatially unresolved (but spectrally resolved) observations of gaseous emission lines<sup>22,25,26</sup> or very low dispersion interferometric measurements<sup>17</sup>.

The finding that gaseous emission, and  $\text{Br}\gamma$  emission in particular, lies within the edge of the dusty component in protoplanetary disks contrasts with previous interferometric studies of young stars. Previous work found the  $\text{Br}\gamma$  emission to lie at radii equal to or larger than the dust, implying an origin of the emission in an outflowing wind<sup>7,8</sup>. The differing results for MWC 480 and the two previously observed sources may stem from different luminosities of the objects. MWC 480 is orders of magnitude less luminous than MWC 297<sup>15</sup>, for which the  $\text{Br}\gamma$  emission is more extended than the dust emission<sup>7</sup>, and approximately half as luminous as HD 104237<sup>27</sup>, for which the  $\text{Br}\gamma$  and dust emission have comparable size scales<sup>8</sup>.  $\text{Br}\gamma$  emission probably traces both accreting and outflowing components in all of these sources to some extent, but the accretion appears to increasingly dominate the emission for lower-luminosity stars.

The distribution of gas at stellocentric radii  $< 0.1 \text{ AU}$  in the inner disk of MWC 480 shows that material is present in this protoplanetary disk at radii comparable to the semi-major axes of

short-period exoplanets<sup>28</sup>. This finding supports the hypothesis that giant planet migration is halted in resonances with the inner edge of the gaseous disk<sup>4,26</sup>. Future observations of gaseous disk truncation radii in solar-type T Tauri stars will enable direct comparison with exoplanets, which are predominantly found around solar-type stars.

The presence of water vapor in the inner regions of the protoplanetary disk surrounding MWC 480 constrains how water (and other material) is transported in the disk terrestrial zone. Because water beyond the ice-line is in solid form, a concentration gradient tends to push water vapor out of the inner disk; the fact that I observe this inner disk vapor suggests continual replenishment through the sublimation of inwardly migrating icy bodies<sup>9</sup>. Water vapor in disk terrestrial regions may also enable the *in situ* formation of water-rich planets via adsorption of water onto dust grains and subsequent growth of these water-laden grains into planetesimals<sup>10</sup>. Finally, as one of the dominant gaseous opacity sources in the near-IR, water vapor can provide an excellent tracer of the temperature and velocity structure of inner disk gas<sup>25</sup>.

1. Shu, F. H., Adams, F. C. & Lizano, S. Star formation in molecular clouds - Observation and theory. *Ann. Rev. Astron. Astrophys.* **25**, 23–81 (1987).
2. Safronov, V. S. *Evolutsiya Doplanetogo Oblake i Obrazovanie Zemli i Planet; English translation, Evolution of the Protoplanetary Cloud and Formation of the Earth and the Planets*, NASA TTF-677 (Nauka, Moscow, 1969).
3. Raymond, S. N., Quinn, T. & Lunine, J. I. Making other earths: dynamical simulations of terrestrial planet formation and water delivery. *Icarus* **168**, 1–17 (2004).

4. Lin, D. N. C., Bodenheimer, P. & Richardson, D. C. Orbital migration of the planetary companion of 51 Pegasi to its present location. *Nature* **380**, 606–607 (1996).
5. Königl, A. Disk accretion onto magnetic T Tauri stars. *Astrophys. J.* **370**, L39–L43 (1991).
6. Millan-Gabet, R. *et al.* The Circumstellar Environments of Young Stars at AU Scales. In *Protostars and Planets V*, B. Reipurth, D. Jewitt, and K. Keil (eds.), (University of Arizona Press, Tucson), 539–554 (2007).
7. Malbet, F. *et al.* Disk and wind interaction in the young stellar object MWC 297 spatially resolved with AMBER/VLTI. *Astron. Astrophys.* **464**, 43–53 (2007).
8. Tatulli, E. *et al.* Constraining the wind launching region in Herbig Ae stars: AMBER/VLTI spectroscopy of HD 104237. *Astron. Astrophys.* **464**, 55–58 (2007).
9. Ciesla, F. J. & Cuzzi, J. N. The evolution of the water distribution in a viscous protoplanetary disk. *Icarus* **181**, 178–204 (2006).
10. Drake, M. J. Origin of water in the terrestrial planets. *Meteoritics and Planetary Science* **40**, 519 (2005).
11. Eisner, J. A. *et al.* Stellar and Molecular Radii of a Mira Star: First Observations with the Keck Interferometer Grism. *Astrophys. J.* **654**, L77–L80 (2007).
12. Colavita, M. M. & Wizinowich, P. L. Keck Interferometer update. In *Interferometry for Optical Astronomy II*. Edited by Wesley A. Traub. *Proceedings of the SPIE*, Volume 4838, 79–88 (2003).

13. Colavita, M. *et al.* Observations of DG Tauri with the Keck Interferometer. *Astrophys. J.* **592**, L83–L86 (2003).
14. Mannings, V., Koerner, D. W. & Sargent, A. I. A rotating disk of gas and dust around a young counterpart to beta Pictoris. *Nature* **388**, 555–557 (1997).
15. Eisner, J. A., Lane, B. F., Hillenbrand, L., Akeson, R. & Sargent, A. Resolved Inner Disks Around Herbig Ae/Be Stars. *Astrophys. J.* **613**, 1049–1071 (2004).
16. Monnier, J. D. *et al.* Few Skewed Disks Found in First Closure-Phase Survey of Herbig Ae/Be Stars. *Astrophys. J.* **647**, 444–463 (2006).
17. Eisner, J. A., Chiang, E. I., Lane, B. F. & Akeson, R. L. Spectrally Dispersed K-Band Interferometric Observations of Herbig Ae/Be Sources: Inner Disk Temperature Profiles. *Astrophys. J.* **657**, 347–358 (2007).
18. Osterbrock, D. E. *Astrophysics of gaseous nebulae and active galactic nuclei* (University Science Books, CA, 1989).
19. Isella, A. & Natta, A. The shape of the inner rim in proto-planetary disks. *Astron. Astrophys.* **438**, 899–907 (2005).
20. Ludwig, C. B. Measurements of the curves-of-growth of hot water vapor. *Applied Optics* **10**, 1057–1073 (1971).
21. Pollack, J. B. *et al.* Composition and radiative properties of grains in molecular clouds and accretion disks. *Astrophys. J.* **421**, 615–639 (1994).



22. Najita, J., Carr, J. S. & Tokunaga, A. T. High-Resolution Spectroscopy of BR gamma Emission in Young Stellar Objects. *Astrophys. J.* **456**, 292 (1996).
23. Calvet, N. & Gullbring, E. The Structure and Emission of the Accretion Shock in T Tauri Stars. *Astrophys. J.* **509**, 802–818 (1998).
24. Muzerolle, J., D'Alessio, P., Calvet, N. & Hartmann, L. Magnetospheres and Disk Accretion in Herbig Ae/Be Stars. *Astrophys. J.* **617**, 406–417 (2004).
25. Carr, J. S., Tokunaga, A. T. & Najita, J. Hot H<sub>2</sub>O Emission and Evidence for Turbulence in the Disk of a Young Star. *Astrophys. J.* **603**, 213–220 (2004).
26. Najita, J. R., Carr, J. S., Glassgold, A. E. & Valenti, J. A. Gaseous Inner Disks. In *Protostars and Planets V*, B. Reipurth, D. Jewitt, and K. Keil (eds.), (University of Arizona Press, Tucson), 507–522 (2007).
27. van den Ancker, M. E., de Winter, D. & Tjin A Djie, H. R. E. HIPPARCOS photometry of Herbig Ae/Be stars. *Astron. Astrophys.* **330**, 145–154 (1998).
28. Marcy, G. *et al.* Observed Properties of Exoplanets: Masses, Orbits, and Metallicities. *Progress of Theoretical Physics Supplement* **158**, 24–42 (2005).
29. Dullemond, C. P., Dominik, C. & Natta, A. Passive Irradiated Circumstellar Disks with an Inner Hole. *Astrophys. J.* **560**, 957–969 (2001).
30. Shu, F. *et al.* Magnetocentrifugally driven flows from young stars and disks. 1: A generalized model. *Astrophys. J.* **429**, 781–796 (1994).

**Acknowledgements** Data presented herein were obtained at the W.M. Keck Observatory from telescope time allocated to the National Aeronautics and Space Administration through the agency’s scientific partnership with the California Institute of Technology and the University of California. The Observatory was made possible by the generous financial support of the W.M. Keck Foundation. I thank the entire Keck Interferometer team for their invaluable contributions to these observations. I also acknowledge input into this work (and this manuscript) from R. Akeson, E. Chiang, A. Glassgold, J. Graham, J. Najita, and R. White. The author is supported by a Miller Research Fellowship.

**Competing Interests** The author declares that he has no competing financial interests.

**Correspondence** Correspondence and requests for materials should be addressed to J.A.E. (email: [jae@astro.berkeley.edu](mailto:jae@astro.berkeley.edu)).

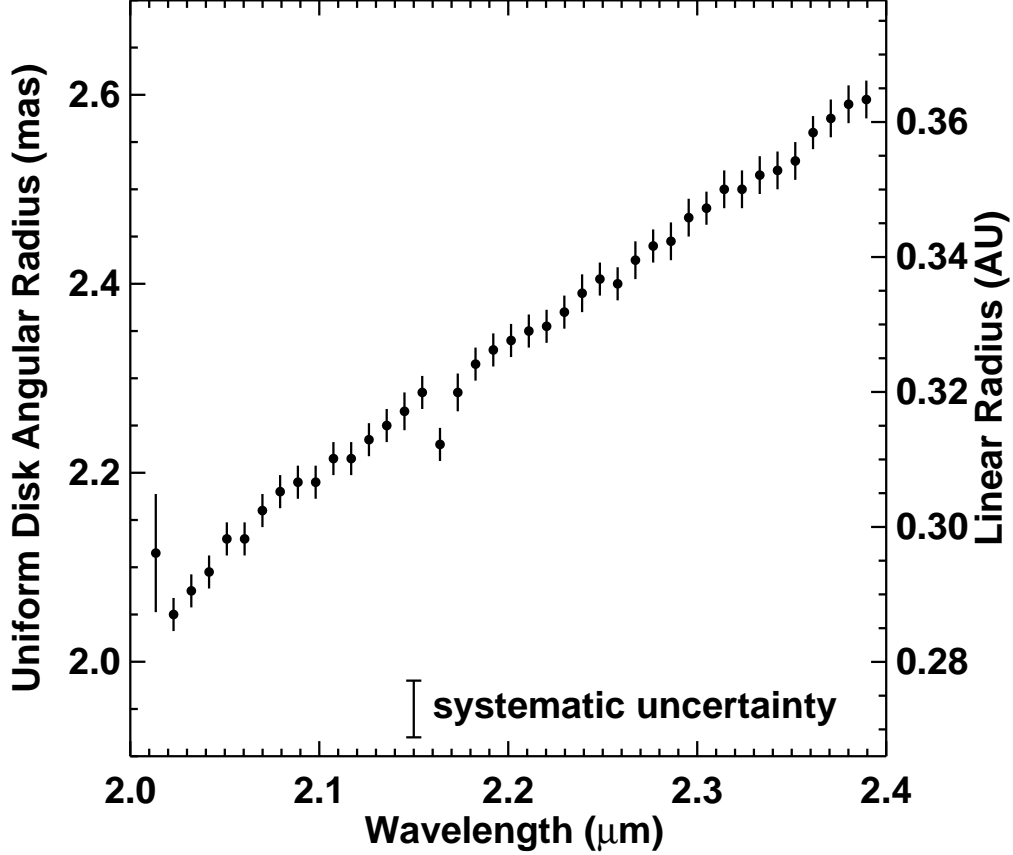


**Fig. 1. Angular size of the near-IR emission from MWC 480 as a function of wavelength.**

Sizes are calculated from squared visibility measurements ( $V^2$ ) made with the Keck Interferometer grism on 12 Nov 2006. The  $V^2$  (and fluxes; see Fig. 2), were calibrated using observations of unresolved stars of known spectral type and parallax<sup>11</sup>. I applied these calibrations to unresolved “check stars” to test the calibration, and thereby estimated channel-to-channel uncertainties ( $1\sigma$  standard deviation) in my flux and  $V^2$  measurements of 3%. The shortest-wavelength data point has a larger uncertainty, because atmospheric water vapor absorption leads to lower photon counts in this channel; I estimate the uncertainty in this channel at  $\sim 10\%$ . There is also a systematic uncertainty of approximately 5% in the overall normalization of the data, due to errors in the absolute calibration<sup>11</sup>. I assume that the emission morphology is a uni-

form disk, for which the measured  $V^2$  are related to the angular diameter of the source,  $\theta_{\text{UD}}$ , by  $V^2 = \{J_1(\pi\theta_{\text{UD}}B_{\text{proj}}/\lambda)/(\pi\theta_{\text{UD}}B_{\text{proj}}/\lambda)\}^2$ , where  $B_{\text{proj}}$  is the projected baseline separation of the two telescopes as seen by the source,  $\lambda$  is the wavelength, and  $J_1$  is a first-order Bessel function. I remove the stellar contribution to the visibilities<sup>15</sup>, and the plotted sizes thus represent only the circumstellar emission. The angular size increases from 2.0 to 2.4  $\mu\text{m}$ , indicating multiple emission components: hot gas at small stellocentric radii and warm dust at larger radii<sup>17</sup>. In addition, the angular size is smaller at 2.165  $\mu\text{m}$ , the wavelength where hot hydrogen gas emits in the  $\text{Br}\gamma$  line, than at adjacent continuum wavelengths.

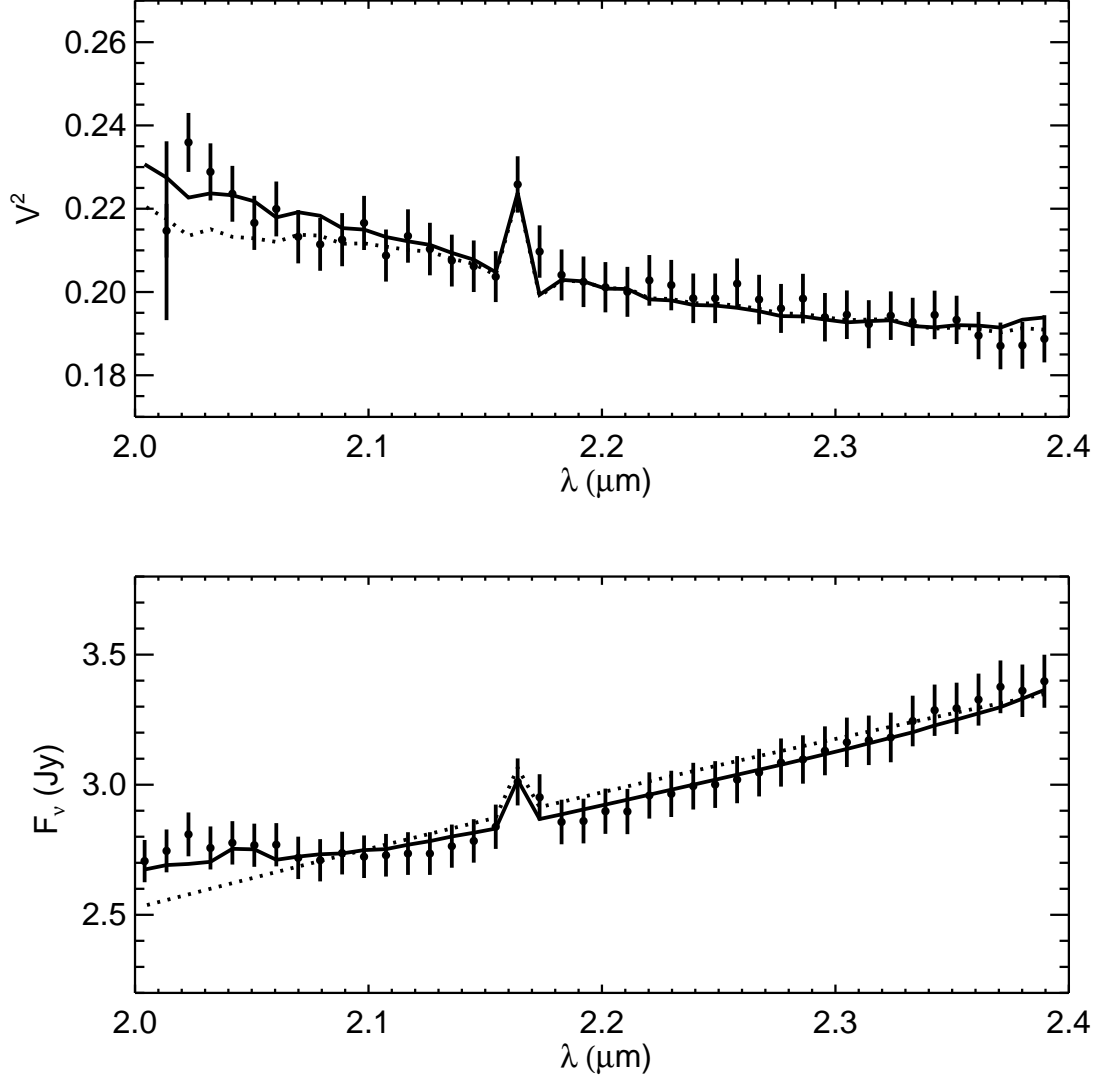


**Fig. 2. Measured  $V^2$  and fluxes, compared to the predictions of simple physical models.**

Plotted error bars indicate estimated  $1\sigma$  (standard deviation) uncertainties of 3%; as noted above, the uncertainty in the shortest wavelength  $V^2$  measurement is larger, approximately 10%. The dotted line shows the values computed for a model including continuum emission from warm dust and hot gas, and  $\text{Br}\gamma$  emission from hydrogen. This model reproduces the overall slopes seen in the data as well as the feature at 2.165  $\mu\text{m}$ , but deviates from the data between 2.0 and 2.1  $\mu\text{m}$ . Hot water vapor contributes significant emission at these wavelengths<sup>20</sup>, and the solid line shows

the predictions of a model that includes  $\text{H}_2\text{O}$ . Because the  $\text{H}_2\text{O}$  emission lies at a radius only slightly larger than that of the hot gaseous continuum, its effect on the visibilities is more subtle than its effect on the measured fluxes. Absorption due to terrestrial atmospheric water vapor affects the data in the shortest-wavelength channel, but not substantially in longer-wavelength channels since, in contrast to the hot water vapor in our model, water vapor at atmospheric temperature and pressure conditions lacks substantial opacity at these wavelengths<sup>20</sup>. The model including  $\text{H}_2\text{O}$  fits the data well over the entire observed wavelength range, and yields substantially smaller residuals between model and data than the model without water vapor. We note that the inferred sizes of the emission components in our model are smaller than the uniform disk sizes plotted in Figure 1; this is due primarily to the different characteristic sizes for uniform disk and relatively narrower ring models<sup>15</sup>. Additional details of the modeling and fitting procedure can be found in previous work<sup>17</sup>.

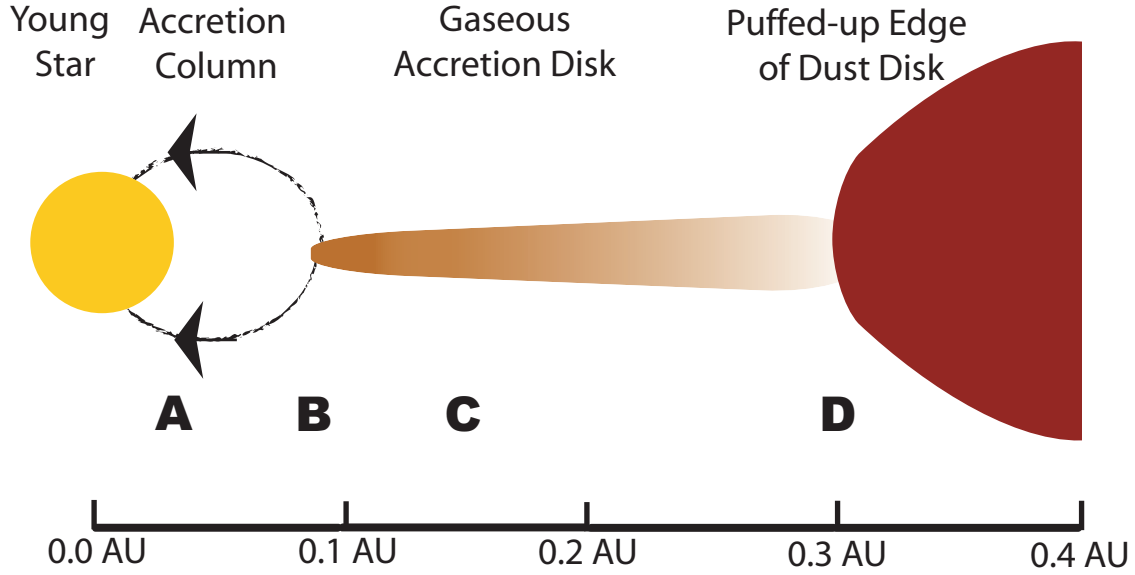


**Fig. 3. The environment within 1 AU of the young star MWC 480.** Dust in the inner disk around MWC 480 extends inward to approximately 0.3 AU (**D**), where the disk temperature becomes high enough to sublimate the dust. The ring-like appearance of the dust sublimation front is compatible with my data, and with physical models predicting a puffed-up and curved inner edge<sup>19,29</sup>. Interior to the dust sublimation radius, gaseous material continues to accrete onto the young star (and may also be blown away in a tenuous wind<sup>30</sup>, which is not depicted). Based on a sketch for a similar young star<sup>24</sup>, I have portrayed a continuous gaseous disk whose optical depth increases at smaller radii. I observe hot continuum emission from the hottest, densest gaseous material at stellocentric radii smaller than 0.1 AU (**B**) and spectral-line emission from hot water vapor at slightly larger radii (**C**). Finally, I observe Br $\gamma$  emission at radii smaller than 0.1 AU, which traces hydrogen gas at high temperatures ( $\sim 10^4$  K). I speculate that this emission arises in the hot accretion shock where infalling gas impacts the stellar surface (**A**). The  $\sim 1$  mas angular resolution of my observations translates into a spatial resolution of approximately 0.1 AU at the distance to MWC 480.